Available online at www.sciencedirect.com
ScienceDirect
Journal of Hazardous Materials 143 (2007) 386–395
Journal of Hazardous Materials
www.elsevier.com/locate/jhazmat

Adsorptive removal of Auramine-O: Kinetic and equilibrium study

Indra Deo Mall [a,*], Vimal Chandra Srivastava [b], Nitin Kumar Agarwal [a]

[a] *Department of Chemical Engineering, Indian Institute of Technology Roorkee, Roorkee 247667, India*
[b] *Department of Chemical Engineering and Technology, Institute of Technology, Banaras Hindu University, Varanasi 221005, India*

Received 1 March 2005; received in revised form 18 July 2006; accepted 15 September 2006
Available online 24 September 2006

Abstract

Present study deals with the adsorption of Auramine-O (AO) dye by bagasse fly ash (BFA) and activated carbon-commercial grade (ACC) and laboratory grade (ACL). BFA is a solid waste obtained from the particulate collection equipment attached to the flue gas line of the bagasse fired boilers of cane sugar mills. Batch studies were performed to evaluate the influences of various experimental parameters like initial pH (pH_0), contact time, adsorbent dose and initial concentration (C_0) for the removal of AO. Optimum conditions for AO removal were found to be $pH_0 \approx 7.0$ and equilibrium time ≈30 min for BFA and ≈120 min for activated carbons. Optimum BFA, ACC and ACL dosages were found to be 1, 20 and 2 g/l, respectively. Adsorption of AO followed pseudo-second order kinetics with the initial sorption rate for adsorption on BFA being the highest followed by those on ACL and ACC. The sorption process was found to be controlled by both film and pore diffusion with film diffusion at the earlier stages followed by pore diffusion at the later stages. Equilibrium isotherms for the adsorption of AO on BFA, ACC and ACL were analyzed by Freundlich, Langmuir, Dubinin–Radushkevich, and Temkin isotherm equations using linear correlation coefficient. Langmuir isotherm gave the best correlation of adsorption for all the adsorbents studied. Thermodynamic study showed that adsorption of AO on ACC (with a more negative Gibbs free energy value) is more favoured. BFA which was used without any pretreatment showed high surface area, pore volume and pore size exhibiting its potential to be used as an adsorbent for the removal of AO.

Keywords: Auramine-O; Adsorption; Dye removal; Bagasse fly ash; Activated carbon

1. Introduction

Auramine (4,4′-dimethylaminobenzophenonimide) and its hydrochloride salt are used in the colouring of paper, textiles and leather; also as food dye [1]. International Agency for Research on Cancer included AO among chemicals for which there is sufficient evidence of carcinogenicity in experimental animals [2] due to its bio-transformation to reactive species in target organs of both rats and humans [1]. Auramine-O (AO), a yellow dye, is commonly used in paper mills, textile mills, leather and carpet industry. Presence of dyes is highly persistent as the manufacturers always go for the most stable dye. Most of the dyes bearing wastewaters have high COD to BOD ratio and they offer considerable resistance for their biodegradation due to thermo- and photo-stability of the dyes [3]. Hence, the conventional methods used in sewage treatment, such as primary and secondary treatment systems, are insufficient in removing these contaminants, with the majority of the research in this field conducted using tertiary treatments [4]. The adsorption process provides an attractive alternative treatment, especially if the adsorbent is inexpensive and readily available. Granular activated carbon is the most popular adsorbent and has been used with great success [5], but is expensive. Consequently, many investigators have studied the feasibility of various low cost substances for the removal of dyes. Critical reviews of low cost adsorbents for waste and wastewater treatment have been presented by Pollard et al. [6] and Mall et al. [7].

BFA is a waste collected from the particulate separation equipment attached to the flue gas line of the sugarcane bagasse-fired boilers and has been used as an effective adsorbent for the removal of substances like phenol [8], dyes [9–11] and metals [12] from the wastewaters. This is available in plenty, and almost free of cost from the sugar mills. The present investigation is an attempt to explore the possibility of using BFA to remove AO

* Corresponding author. Tel.: +91 1332 285319; fax: +91 1332 276535/273560.
E-mail addresses: id_mall2000@yahoo.co.in (I.D. Mall), vimalcsr@yahoo.co.in (V.C. Srivastava).

0304-3894/$ – see front matter © 2006 Elsevier B.V. All rights reserved.
doi:10.1016/j.jhazmat.2006.09.059

from aqueous solutions. The efficacy of BFA in removing AO is also compared with those of activated carbons. Two types of activated carbons, namely the commercial grade available in the free market (ACC) and the laboratory grade (ACL) have been used in the present study. The present study reports the effect of such factors as the initial pH (pH_0), adsorbent dose (m), initial AO concentration (C_0) and contact time (t) on the adsorption efficiency of AO on BFA and the activated carbons. The kinetics of adsorption of AO on three adsorbents were analyzed by fitting various kinetic models, viz. pseudo-first-order, pseudo-second-order, Bangham and intra-particle diffusion models with the experimental data. The equilibrium sorption capacity of AO on the three adsorbents was studied using various isotherm equations.

2. Material and methods

2.1. Adsorbents and their characterisation

BFA was obtained from U.P. State Sugar Corporation Ltd., Doiwala Unit, Dehradun, India. The commercial grade activated carbon (ACC) manufactured by Rajasthan Breweries Ltd. was procured from the open market (Kharibaoli, Delhi) and the laboratory grade activated carbon (ACL) manufactured by GSE Chemical Testing Laboratory and Allied Industry, New Delhi was procured from local suppliers. The adsorbents were used as procured. The detailed physico-chemical characteristics of the adsorbents have already been presented elsewhere [8,10,12].

The point of zero charge (pH_{pzc}) of the adsorbents were determined by the solid addition method [13]. To a series of 100 ml conical flasks 45 ml of KNO_3 solution of known strength was transferred. The pH_0 values of the solution were roughly adjusted from 2 to 12 by adding either 0.1 N HNO_3 or NaOH. The total volume of the solution in each flask was made exactly to 50 ml by adding the KNO_3 solution of the same strength. The pH_0 of the solutions were then accurately noted, and 0.1 g of adsorbent was added to each flask, which were securely capped immediately. The suspensions were then manually shaken and allowed to equilibrate for 48 h with intermittent manual shaking. The pH values of the supernatant liquid were noted. The difference between the initial and final pH (pH_f) values ($\Delta pH = pH_0 - pH_f$) was plotted against the pH_0. The point of intersection of the resulting curve at which $\Delta pH = 0$ gave the pH_{pzc}. The procedure was repeated for different concentrations of KNO_3.

2.2. Adsorbate

The adsorbate AO dye [C.I. = 41000, molecular formula $(CH_3)_2NC_6H_4$ (C:NH) $C_6H_4N(CH_3)_2$: HCl, FW = 298.80, λ_{max} = 432 nm] was supplied by the S.D. Fine Chemicals, Mumbai, India. The structure of AO is illustrated in Fig. 1. An accurately weighed quantity of the dye was dissolved in distilled water to prepare stock solution (100 mg/l). Experimental solutions of desired concentration were obtained by successive dilutions.

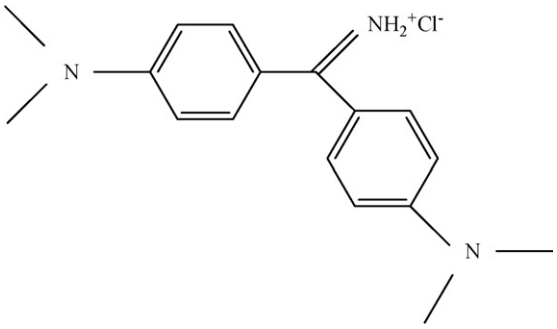

Fig. 1. Molecular structure of Auramine-O dye.

2.3. Analytical measurements

Concentrations of AO were determined by finding out the absorbance at the characteristic wavelength using a double beam UV–vis spectrophotometer (Shimadzu, Japan; model UV 210 A). A standard solution of the dye was taken and the absorbance was determined at different wavelengths to obtain a plot of absorbance versus wavelength. The wavelength corresponding to maximum absorbance (λ_{max}) as determined from this plot was 432 nm. This wavelength was used for preparing the calibration curve between absorbance and the concentration of the dye solution. The calibration plot showed a linear variation up to 20 mg/l concentration. Therefore, the samples with higher concentration of AO (>20 mg/l) were diluted with distilled water, whenever necessary, to make the concentration less than 20 mg/l, for the accurate determination of the AO concentration with the help of the linear portion of the calibration curve.

2.4. Batch experimental programme

For each experimental run, 50 ml of AO solution of known C_0, pH_0 and a known amount of the adsorbent were taken in a 100 ml stoppered conical flask. This mixture was agitated in a temperature-controlled shaking water bath at a constant speed of 150 rpm at 30 ± 1 °C. Samples were withdrawn at appropriate time intervals. Some adsorbents particles remain suspended and do not settle down easily. Therefore, all the samples were centrifuged (Research Centriguge, Remi scientific works, Mumbai) at 5000 rpm for 30 min and analyzed for the residual dye concentration using double beam UV–vis spectrophotometer.

The effect of pH_0 on dye removal was studied over a pH_0 range of 3–12. pH_0 was adjusted by the addition of dilute aqueous solutions of HCI or NaOH (0.10 M). For the optimum amount of adsorbent per unit mass of adsorbate, a 50 ml dye solution was contacted with different amounts of adsorbents till equilibrium was attained. The kinetics of adsorption was determined by analyzing adsorptive uptake of the dye from the aqueous solution at different time intervals. For adsorption isotherms, dye solutions of different concentrations were agitated with the known amount of adsorbent till the equilibrium was achieved. The residual dye concentration (C) of the solution was then determined.

The percentage removal of AO and equilibrium adsorption uptake, q_e (mg/g), was calculated using the following

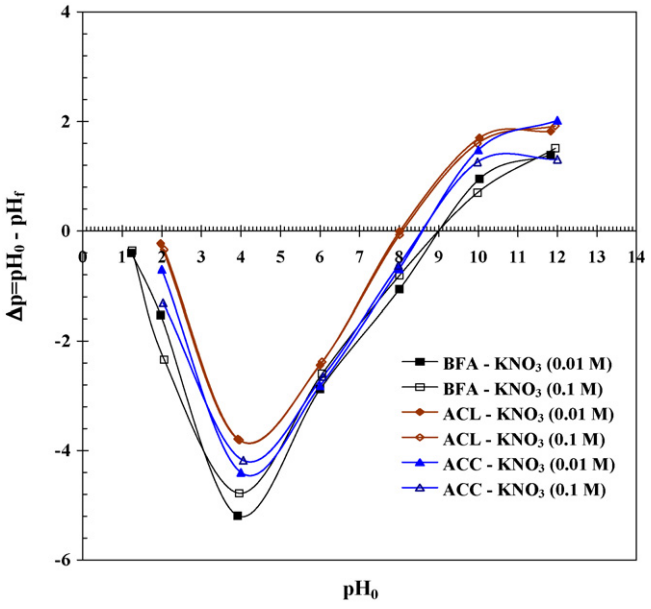

Fig. 2. Point of zero charge (pH_{pzc}) of adsorbents.

relationships:

$$\%\ \text{removal} = 100 \times \frac{C_0 - C_e}{C_0}, \quad (1)$$

$$\text{amount adsorbed, } q_e = \frac{C_0 - C_e}{m}, \quad \text{(mg of adsorbate/g of adsorbent)} \quad (2)$$

where C_e is the equilibrium AO concentration (mg/l).

3. Results and discussion

3.1. Effect of initial pH (pH_0)

To understand the adsorption mechanism, it is necessary to determine the point of zero charge (pH_{pzc}) of the adsorbent. Adsorption of cations is favoured at $pH > pH_{pzc}$, while the adsorption of anions is favoured at $pH < pH_{pzc}$. The specific adsorption of cations shifts pH_{pzc} towards lower values, whereas the specific adsorption of anions shifts pH_{pzc} towards higher values. Fig. 2 shows that for all the concentrations of KNO_3, the zero value of ΔpH and hence, pH_{pzc} for BFA, ACC and ACL lies at the pH_0 value of 9.0, 8.5 and 8.1, respectively.

pH is known to affect the structural stability of dyes and, therefore, its colour intensity [9,10]. Hence the effect of pH_0 was studied with blank dye solutions of $C_0 = 10$ mg/l. The solution was kept for 1 h after the pH adjustment and, thereafter, the absorbance of the solution was found out. It was found that the colour is stable at pH_0 around 7. Fig. 3 also shows the plot for the colour removal of AO due to pH change over a pH_0 range of 3–11. The colour intensity remains stable below pH_0 7 and becomes unstable in the basic range. Colour removal due to pH change alone may be due to the structural changes taking place in the dye molecules [10].

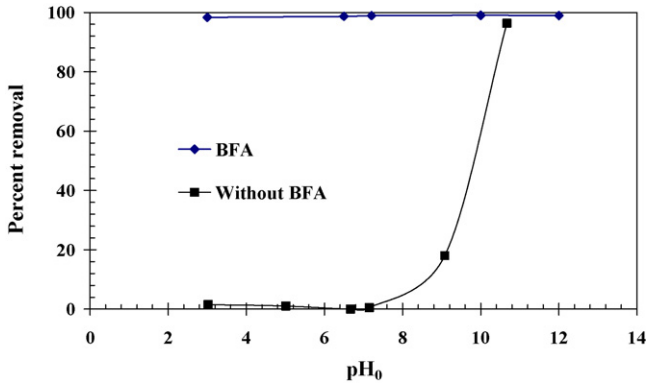

Fig. 3. Effect of pH_0 on the adsorption of Auramine-O by bagasse fly ash ($T = 30\,^{\circ}C$, $t = 3$ h, and $C_0 = 10$ mg/l, BFA dosage = 1 g/l).

Effect of pH_0 for the removal of AO by BFA is shown in Fig. 3 for $C_0 = 10$ mg/l, $t = 3$ h and $m = 1$ g/l. The removal of the cationic dye AO increases very marginally with the increase in pH. At higher pH, the association of dye cations with the more negative charged sites of the BFA could easily take place thereby increasing cationic dye removal.

$$MO^- + dye^+ \rightleftharpoons M\text{–}O\text{–}dye$$

where M stands for aluminium, calcium, silica, etc. present in the BFA [11]. Further studies on adsorptive removal of AO by BFA were carried out at a pH_0 7.0.

3.2. Effect of adsorbent dosage (m)

The effect of m on the removal of AO by BFA, ACC and ACL at $C_0 = 10$ mg/l is shown in Fig. 4. This figure reveals that the removal of AO increases with increase in adsorbent dosage. An increase in the adsorption with the adsorbent dosage can be attributed to greater surface area and the availability of more adsorption sites. The removal of AO at adsorbent dosage larger than optimum m (m_{opt}) remains almost unchanged. m_{opt} values for BFA, ACC and ACL were found to be 1, 20 and 2 g of adsorbent per litre of dye solution, respectively.

At small m, the adsorbent surface become saturated with AO and the residual concentration in the solution is large. With

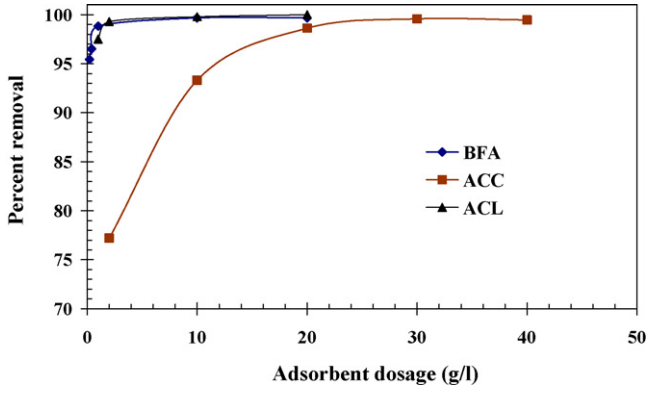

Fig. 4. Effect of adsorbent dosage on the adsorption of Auramine-O by various adsorbents (pH_0 7.0, $T = 30\,^{\circ}C$, $t = 3$ h, and $C_0 = 10$ mg/l).

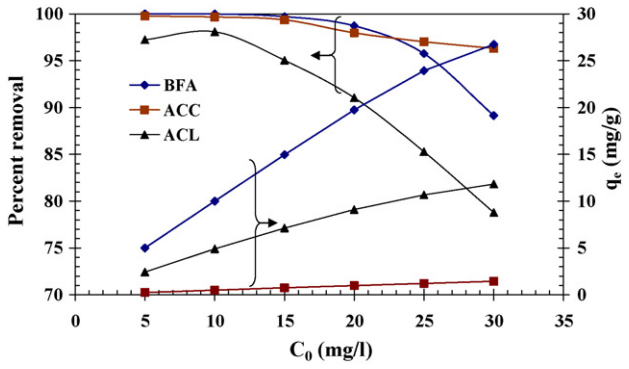

Fig. 5. Effect of C_0 for the removal of Auramine-O by various adsorbents (pH$_0$ 7.0, T = 30 °C, and t = 3 h, BFA dosage = 1 g/l, ACC dosage = 20 g/l, and ACL dosage = 2 g/l).

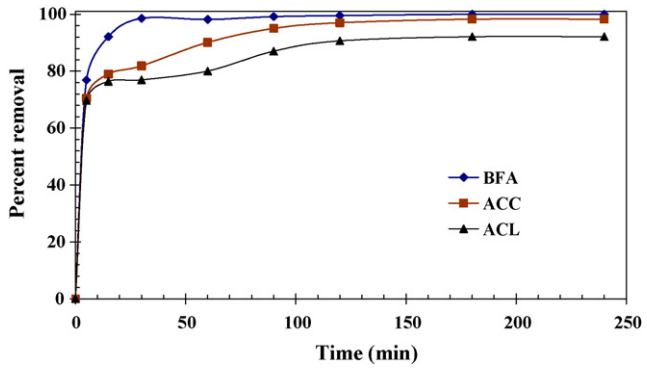

Fig. 6. Effect of t on the removal of Auramine-O by various adsorbents (pH$_0$ 7.0, T = 30 °C, and C_0 = 10 mg/l, BFA dosage = 1 g/l, ACC dosage = 20 g/l, and ACL dosage = 2 g/l).

increase in the m, the AO removal increases due to increased AO uptake by the increases amount of adsorbent. At $m \leq m_{opt}$, the incremental AO removal becomes very low, as the surface AO concentration and the solution AO concentration come to equilibrium with each other. At about $m = m_{opt}$, the removal efficiency becomes almost constant. There is very little difference between the AO uptake by ACL and BFA.

3.3. Effect of initial dye concentration (C_0)

The effect of C_0 on the removal of AO by different adsorbents is shown in Fig. 5. From the figure, it is evident that the percent AO removal decreased with the increase in C_0, although, amount of AO adsorbed per unit mass of adsorbent (q_e) increased with the increase in C_0. The q_e increased with the increase in C_0 as the resistance to the uptake of AO from the solution decreases with the increase in AO concentration. The rate of adsorption also increases with the increase in C_0 due to increase in the driving force.

3.4. Effect of contact time (t)

Effect of contact time for the removal of AO by the adsorbents at respective optimum dosages showed rapid adsorption of dye in the first 15 min and, thereafter, the adsorption rate decreased gradually (Fig. 6). The adsorption of AO reached equilibrium in about 30 min and 120 min for adsorption onto BFA; activated carbons, respectively. In the initial stage of sorption, a large number of vacant surface sites are available for adsorption. After lapse of some time, the remaining vacant surface sites are difficult to be occupied due to repulsive forces between the solute molecules on the solid surface and the bulk phase. Besides, the dye molecules are adsorbed into the mesopores that get almost saturated with dye ions during the initial stage of adsorption. Thereafter, the dye molecules have to traverse farther and deeper into the pores encountering much larger resistance. This results in the slowing down of the adsorption during the later period of adsorption. Aggregation of dye molecules with the increase in contact time also makes it almost impossible to diffuse deeper into the adsorbent structure at highest energy sites. This aggregation negates the influence of contact time as the mesopores get filled up and start offering resistance to diffusion of aggregated dye molecules in the adsorbents. This is the reason why equilibrium is reached in 30 min and 120 min only for adsorption onto BFA; activated carbons, respectively. The difference in equilibrium time may be due to the difference in the particle size and pore area of the adsorbents. Since activated carbons have higher percentage of micro-pore area, therefore, they require greater equilibrium contact time. The adsorption curves were single, smooth and continuous leading to saturation and indicated the possible monolayer coverage on the surface of adsorbents by the dye molecules [14]. The curved portion of these graphs is due to surface mass transfer and final linear part is due to intra-particle diffusion.

3.5. Adsorption kinetic study

In order to investigate the adsorption processes of AO on BFA, ACC and ACL, four kinetic models viz. pseudo-first-order, pseudo-second-order, Bangham and intra-particle diffusion models were used.

3.5.1. Pseudo-first-order model

The sorption of molecules from a liquid phase to a solid phase can be considered as a reversible process with equilibrium being established between the solution and the solid phase. Assuming a non-dissociating molecular adsorption of dye ions on adsorbents, the sorption phenomenon can be described as the diffusion controlled process [8].

$$\mathrm{A} + \mathrm{S} \underset{k_D}{\overset{k_A}{\rightleftharpoons}} \mathrm{A.S.} \tag{3}$$

where A is the adsorbate, S the active site on the adsorbent and A.S. is the activated complex. k_A and k_D are the adsorption and desorption rate constants, respectively. Using first order kinetics it can be shown that with no adsorbate initially present on the adsorbent (i.e. $C_{A.S.0} = 0$ at $t = 0$), the fractional uptake of the adsorbate by the adsorbent can be expressed as

$$\frac{q}{q_e} = 1 - \exp\left[k_A C_S + \frac{k_A}{K_S}\right] t \tag{4}$$

Table 1
Kinetic parameters for the removal of Auramine-O by various adsorbents

Adsorbent	$q_{e,exp}$ (mg/g)	$q_{e,calc}$ (mg/g)	k_f (min^{-1})	R^2
Pseudo-first-order model				
BFA	10.000	1.773	0.0304	0.9282
ACC	0.492	0.159	0.0228	0.9193
ACL	4.608	1.380	0.0212	0.9096
Adsorbent	$q_{e,calc}$ (mg/g)	h (mg/g min)	k_S (g/mg min)	R^2
Pseudo-second-order model				
BFA	10.081	5.4674	0.0539	1
ACC	0.502	0.0966	0.3830	0.9993
ACL	4.704	0.6978	0.0395	0.9989
Adsorbent	k_0 (g)	α		R^2
Bangham model				
BFA	40.6316	0.3791		0.9525
ACC	0.7082	0.2986		0.9101
ACL	7.9329	0.1935		0.8608
Adsorbent	$k_{id,1}$ (mg/g min$^{1/2}$)	I_1 (mg/g)		R^2
Intra-particle diffusion model				
BFA	2.8789	1.2507		1
ACC	0.1302	0.0619		1
ACL	1.6438	−0.1927		1
Adsorbent	$k_{id,2}$ (mg/g min$^{1/2}$)	I_2 (mg/g)		R^2
Intra-particle diffusion model				
BFA	0.0733	9.0286		0.7985
ACC	0.0090	0.3689		0.9039
ACL	0.0806	3.4886		0.9024

where q_e is the fraction of the adsorbate adsorbed on the adsorbent under equilibrium condition, $K_S = K_A/K_D$, and C_S is the adsorbent concentration in the solution.

Eq. (4) can be transformed as

$$\log(q_e - q_t) = \log q_e - \frac{k_f}{2.303}t \quad (5)$$

where

$$k_f = \left(k_A C_S + \frac{k_A}{K_S}\right); \quad (6)$$

Table 1 presents the values of adsorption rate constant (k_f) as determined from the plot of $\log(q_e - q_t)$ against t (not shown here). Value of k_f is 0.0304, 0.0228 and 0.0212 min^{-1}, respectively, for AO adsorption on BFA, ACC and ACL. These values indicate that the removal is fastest on BFA among the three adsorbents.

3.5.2. Pseudo-second-order model

The pseudo-second-order model can be represented in the following form [15]:

$$\frac{dq_t}{dt} = k_S(q_e - q_t)^2 \quad (7)$$

where k_S is the pseudo-second-order rate constant (g/mg min). The integration of Eq. (7) with the boundary conditions, $q_t = 0$ at $t = 0$ and $q_t = q_t$ at $t = t$, results in the following equation:

$$\frac{t}{q_t} = \frac{1}{k_S q_e^2} + \frac{1}{q_e}t \quad (8)$$

The initial sorption rate, h (mg/g min), at $t \to 0$ can be defined as

$$h = k_S q_e^2 \quad (9)$$

q_e is obtained from the slope of the t/q_t versus t plot (Fig. 7) and h is obtained from the intercept. Since q_e is known from the slope, k_S can be determined from the value of h. The best-fit values of h, q_e and k_S along with the correlation coefficients for the pseudo-first-order and pseudo-second-order models are shown in Table 1. The $q_{e,exp}$ and the $q_{e,cal}$ values for the pseudo-first-order model and pseudo-second-order models are also shown in Table 1. The $q_{e,exp}$ and the $q_{e,cal}$ values from the pseudo-second-order kinetic model are very close to each other. The calculated correlation coefficients are also closer to unity for pseudo-second-order kinetics than that for the pseudo-first-order kinetic model. Therefore, the sorption can be approximated more appropriately by the pseudo-second-order kinetic model than the first-order kinetic model for the adsorption of AO ions onto BFA, ACC and ACL. Experimental results did not follow pseudo-first-order kinetics as there was difference in two important aspects: (i) $k_f(q_e - q_t)$ does not represent the number of available sites and (ii) $\log q_e$ was not equal to the intercept of the plot of $\log(q_e - q_t)$ against t. It can be seen that the initial sorption rate (h value) is highest for adsorption of AO on BFA.

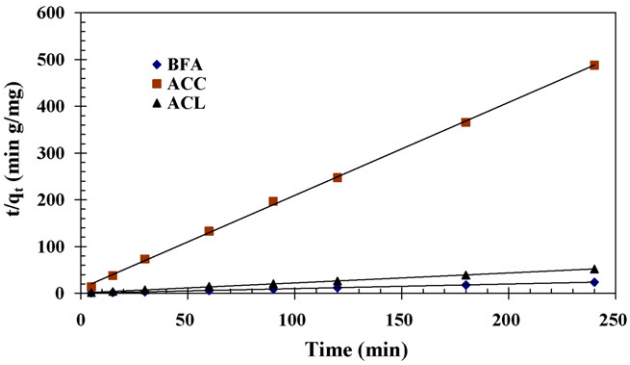

Fig. 7. Pseudo-second-order kinetic plots for the removal of Auramine-O by various adsorbents (pH$_0$ 7.0, $T = 30\,^{\circ}$C, and $C_0 = 10$ mg/l, BFA dosage = 1 g/l, ACC dosage = 20 g/l, and ACL dosage = 2 g/l).

Table 2 shows the values of the values of k_f and k_S along with the $q_{e,exp}$ and the $q_{e,cal}$ values from the pseudo-first-order and pseudo-second-order kinetic models for the adsorption of various dyes onto activated carbon and other adsorbents. Wide variation is seen in the data with minimum value of k_f being 0.012 min^{-1} for orange-G adsorption onto BFA [11] and the maximum value being of 0.301 min^{-1} for methylene blue adsorption onto commercial activated carbon [17]. Similarly, wide variation is observed for k_S values. This wide variation in k_f and k_S values is expected owing to the wide variation in experimental conditions, and different nature of adsorbate–adsorbent systems. However, the $q_{e,exp}$ and the $q_{e,cal}$ values from the pseudo-second-order kinetic model are, generally, very close

Table 2
Kinetic model constants for adsorption of dyes on various adsorbents

Adsorbent	Adsorbate	pH	T (°C)	C_0 (mg/l)	m (g/l)	t_{eq}	$q_{e,exp}$	$q_{e,cal}$ (f)	k_f (min^{-1})	$q_{e,cal}$ (s)	k_S (g/mg min)	$k_{id,1}$	$k_{id,2}$	Reference
BFA	MG	7.0	30	10	1	240	9.971	0.212	0.017	9.980	0.394	0.007	-	[9]
ACC	MG	7.0	30	10	20	240	0.500	0.052	0.024	0.502	1.977	0.002	-	[9]
ACL	MG	7.0	30	10	4	240	2.500	0.260	0.012	2.506	0.237	0.014	-	[9]
BFA	CR	7.0	30	10	1	240	9.853	2.073	0.016	9.638	0.061	0.291	0.041	[10]
ACC	CR	7.0	30	10	20	240	0.496	0.203	0.013	0.477	0.413	0.024	0.008	[10]
ACL	CR	7.0	30	10	2	240	4.819	1.471	0.022	4.789	0.069	0.243	0.024	[10]
BFA	OG	4.0	30	10	2	240	3.881	1.245	0.012	3.765	0.128	0.177	0.029	[11]
BFA	MV	9.0	30	10	4	240	9.768	3.712	0.022	9.711	0.023	0.307	0.060	[11]
BFA	BG	3.0	30	50	3	300	16.664	1.176	0.019	16.666	0.141	0.134	0.010	[16]
BFA	BG	3.0	30	100	3	300	33.089	4.009	0.026	33.223	0.043	0.472	0.017	[16]
BFA	BG	3.0	30	200	3	300	65.929	10.139	0.015	65.789	0.010	1.043	0.183	[16]
CAC	MB	7.4	30	600	2	35	–	–	0.301	–	–	1.441	–	[17]
BDC	MB	7.4	30	100	10	35	–	–	0.225	–	–	0.373	–	[17]
CSC	MB	7.4	30	100	10	35	–	–	0.262	–	–	0.295	–	[17]
GSC	MB	7.4	30	100	10	35	–	–	0.243	–	–	0.246	–	[17]
RHC	MB	7.4	30	200	10	35	–	–	0.332	–	–	0.273	–	[17]
SC	MB	7.4	30	200	10	35	–	–	0.344	–	–	0.364	–	[17]
CAC	CR	7.4	30	50	4.6	35	–	–	0.139	–	–	0.251	–	[18]
BDC	CR	7.4	30	75	10	35	–	–	0.037	–	–	0.109	–	[18]
CSC	CR	7.4	30	50	10	35	–	–	0.047	–	–	0.223	–	[18]
GSC	CR	7.4	30	75	10	35	–	–	0.029	–	–	0.129	–	[18]
RHC	CR	7.4	30	75	10	35	–	–	0.043	–	–	0.293	–	[18]
SC	CR	7.4	30	75	10	35	–	–	0.051	–	–	0.148	–	[18]
CpAC	CR	2.0	35	20	10	40	3.333	1.180	0.210	3.096	0.830	–	–	[19]

Adsorbent—BFA: bagasse fly ash, ACC: commercial grade activated carbon, ACL: laboratory grade activated carbon, AC: activated carbon, CAC: commercial activated carbon; BDC: bamboo duct carbon, CSC: coconut shell carbon, GSC: groundnut shell carbon, RHC: rice husk carbon; SC: straw carbon, and CpAC: coir-pith activated carbon. Adsorbate—BG: brilliant green, OG: orange-G, MV: methyl violet, CR: congo-red, MG: malachite green, RR 45: reactive red, RG 8: reactive green, AB: astrazine blue, TB: telon blue, and MB: methylene blue.

to each other for every adsorbate–adsorbent system. Therefore, pseudo-second-order kinetic model better approximates the kinetics of dye adsorption onto various adsorbents.

3.5.3. Intra-particle diffusion study

The adsorbate transport from the solution phase to the surface of the adsorbent particles occurs in several steps. The overall adsorption process may be controlled either by one or more steps, e.g. film or external diffusion, pore diffusion, surface diffusion and adsorption on the pore surface, or a combination of more than one step. In a rapidly stirred batch adsorption, the diffusive mass transfer can be related by an apparent diffusion coefficient which will fit the experimental sorption rate data. Generally, a process is diffusion controlled if its rate is dependent upon the rate at which components diffuse towards one another. The possibility of intra-particle diffusion was explored by using the intra-particle diffusion model [20].

$$q_t = k_{id} t^{1/2} + I \tag{10}$$

where k_{id} is the intra-particle diffusion rate constant (mg/g min$^{0.5}$) and I (mg/g) is a constant that gives idea about the thickness of the boundary layer, i.e., larger the value of I the greater is the boundary layer effect [21]. If the Weber and Morris [20] plot of q_t versus $t^{1/2}$ satisfies the linear relationship with the experimental data, then the sorption process is found be controlled by intra-particle diffusion only. However, if the data exhibit multi-linear plots, then two or more steps influence the sorption process. The mathematical dependence of fractional uptake of adsorbate on $t^{1/2}$ is obtained if the sorption process is considered to be influenced by diffusion in the cylindrical (or spherical) and convective diffusion in the adsorbate solution. It is assumed that the external resistance to mass transfer surrounding the particles is significant only in the early stages of adsorption. This is represented by first sharper portion. The second linear portion is the gradual adsorption stage with intra-particle diffusion dominating.

Fig. 8 presents the plots of q_t versus $t^{1/2}$ for all the adsorbates. It is evident from Fig. 8 that adsorption follows two phases, viz. (I) a linear phase in which instantaneous extremely fast uptake takes place and (II) a quasi-stationary state. In phase (I), about

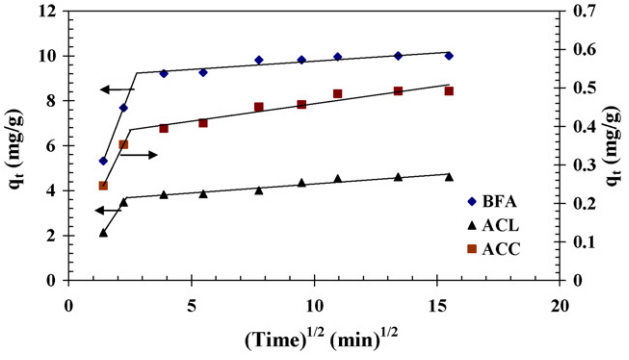

Fig. 8. Weber–Morris intra-particle diffusion plots for the removal of Auramine-O by various adsorbents (pH$_0$ 7.0, T = 30 °C, and C_0 = 10 mg/l, BFA dosage = 1 g/l, ACC dosage = 20 g/l, and ACL dosage = 2 g/l).

80% of AO was uptaken by BFA within a $t^{1/2}$ value of 2.8 min and manifests an average rate of uptake of about 3.1 mg/g min$^{1/2}$. This is attributed to the instantaneous utilization of the most readily available adsorbing sites on the adsorbent surface. In the case of ACC, about 76% of the AO was uptaken within a $t^{1/2}$ value of 2.7 min and manifests an average rate of uptake of about 0.14 mg/g min$^{1/2}$. For AO adsorption on ACL, 74% removal took place within a $t^{1/2}$ value of 2.7 min, manifesting an average rate of uptake of about 1.18 mg/g min$^{1/2}$. Phase (II) may be attributed to a very slow diffusion of the adsorbates from the surface film into the mesopores of the adsorbent.

In Fig. 8, the data points are related by two straight lines—the first straight portion depicts boundary layer diffusion effects or external mass transfer effects [22] while the second linear portion is due to intra-particle or pore diffusion. Extrapolation of the linear portions of the plots back to the *y*-axis gives the intercepts which provide the measure of the boundary layer thickness. The deviation of straight lines from the origin (Fig. 8) may be due to difference in rate of mass transfer in the initial and final stages of adsorption. Further, such deviation of straight line from the origin indicates that the pore diffusion is not the sole rate-controlling step. The slope of the Weber and Morris plots – q_t versus $t^{1/2}$ – are defined as a rate parameter, characteristic of the rate of adsorption in the region where intra-particle diffusion is rate-controlling. The values of rate parameters ($k_{id,1}$ and $k_{id,2}$) as given in Table 1 show that $k_{id,1}$ and $k_{id,2}$ values are, generally, highest for BFA. The values of the correlation coefficients are also given in Table 1. They show that the Weber–Morris model shows better representation of the data than the pseudo-first-order kinetic model.

3.5.4. Bangham's equation

Kinetic data were further used to know about the slow step occurring in the present adsorption system using Bangham's equation [23].

$$\log\log\left(\frac{C_0}{C_0 - q_t m}\right) = \log\left(\frac{k_0 m}{2.303V}\right) + \alpha\log(t) \tag{11}$$

where V is the volume of solution (ml), q_t (mg/g) is the amount of adsorbate retained at t, and α (<1) and k_0 are constants. The double logarithmic plot (not shown here) according to above equation did not yielded perfect linear curves for AO removal by BFA, ACC and ACL showing that the diffusion of adsorbate into pores of the sorbent is not the only rate-controlling step [24]. With increase in the contact time, the effect of diffusion process on overall sorption could be ignored. It may be that both film and pore diffusions are involved in the removal process to different extent. Values of Bangham parameters, correlation coefficient and error function values are given in Table 1.

3.6. Adsorption equilibrium study

To optimize the design of an adsorption system for the removal of adsorption of adsorbates, it is important to establish the most appropriate correlation for the equilibrium curves. Freundlich, Langmuir, Dubinin–Radushkevich, and Temkin isotherm equations have been used to describe the equilibrium nature of adsorption of AO onto BFA, ACC and ACL.

Table 3
Isotherm parameters for removal of Auramine-O by different adsorbents

Adsorbent	K_F ((mg/g)/(mg/l)$^{1/n}$)	$1/n$	R^2
Freundlich constants			
BFA	17.855	0.547	0.9611
ACC	1.431	0.371	0.9025
ACL	7.608	0.254	0.9953
Adsorbent	q_m (mg/g)	K_L (l/mg)	R^2
Langmuir constants			
BFA	31.177	2.019	0.9907
ACC	1.509	8.412	0.9777
ACL	12.552	1.929	0.9957
Adsorbent	K_T (l/mg)	B_1	R^2
Temkin constants			
BFA	27.891	6.025	0.9319
ACC	153.189	0.264	0.9664
ACL	55.577	1.994	0.9953
Adsorbent	q_S (mg/g)	E (kJ/mol)	R^2
D–R constants			
BFA	19.754	4.032	0.8722
ACC	1.342	5.616	0.9423
ACL	10.184	3.709	0.8608

3.6.1. Freundlich and langmuir isotherms

The Freundlich isotherm is derived by assuming a heterogeneous surface with a non-uniform distribution of heat of adsorption over the surface. Whereas in the Langmuir theory the basic assumption is that sorption takes place at specific homogeneous sites within the adsorbent. The adsorption data of AO were correlated with Freundlich and Langmuir models, which are represented by the following equations:

$$\text{Freundlich isotherm} \quad q_e = K_F C_e^{1/n} \quad \text{or}$$

$$\ln q_e = \ln K_F + \frac{1}{n}\ln C_e \tag{12}$$

$$\text{Langmuir isotherm} \quad q_e = \frac{K_L q_m C_e}{1 + K_L C_e}$$

$$\text{or} \quad \frac{C_e}{q_e} = \frac{C_e}{q_m} + \frac{1}{K_L q_m} \tag{13}$$

where K_F is the Freundlich constant (l/mg), $1/n$ the heterogeneity factor, K_L is the Langmuir adsorption constant (l/mg) related to energy of adsorption and q_m signifies adsorption capacity (mg/g).

Freundlich and Langmuir isotherm constants were determined from the plots of $\ln q_e$ versus $\ln C_e$ and C_e/q_e versus C_e (not shown here), respectively, using MS Excel for Windows. Calculated linear correlation coefficients for Freundlich and Langmuir isotherms by using linear regression procedure at 30 °C are shown in Table 3. As seen, Langmuir isotherm

fits better to the experimental data than other isotherms for AO adsorption on any of the three adsorbents. AO adsorption isotherms for BFA and ACL fit better to the isotherm data than ACC. The values of parameters for Freundlich and Langmuir isotherms are given in Table 3.

The mono-component Langmuir constant, q_m, is the monolayer saturation at equilibrium. The other mono-component Langmuir constant, K_L, corresponds to the concentration at which a $q_m/2$ amount of AO is bound and indicates the affinity for the binding of AO. A high K_L value indicates a higher affinity [12]. The obtained data given in Table 3 also indicate that the amount of AO adsorbed on BFA to form a complete monolayer on the surface is higher than activated carbons. A large value of K_L for ACC, however, implies that ACC has the strongest bonding for AO.

K_F and $1/n$, the mono-component Freundlich constants are indicators of adsorption capacity and adsorption intensity, respectively. Higher the value of $1/n$, higher will be the slope expressed by $1/n$ and thus higher the affinity. Moreover, closer the $1/n$ value of Freundlich is to 0 the less heterogeneous is the system. The data obtained in this study (Table 3) indicated that the BFA represents more heterogeneous surface for AO. Table 3 also showed that $1/n < 1$; indicating that all the adsorbents favourably adsorbed AO at pH_0 7.0 [25]. The magnitude of K_F also showed the higher uptake of AO by BFA as compared to ACL and ACC.

Several authors have reported Freundlich and Langmuir constants for adsorption of dyes on various adsorbents. The Freundlich and Langmuir constants values obtained in some of these works, although under different environmental conditions, are given in Table 4. Wide variation is seen in the q_m values. Since the adsorbate concentration range (5–30 mg/l) in the present study are in the lower concentration range, the q_m values are small as compared to other dye–adsorbent systems. This is due to the fact that unit adsorption per gram of adsorbent is higher in the higher dye concentration range and lower in the lower dye concentration range while removal is higher for lower concentration adsorbate solution and lower for higher concentration adsorbate solution. Since, the isotherm parameters differ widely in their values for activated carbons of different origins; hence one should be cautious while using these values in design of adsorption systems.

Table 4
Freundlich and Langmuir constants for adsorption of dyes on various adsorbents

Adsorbent	Adsorbate	pH	T (°C)	C_0 (mg/l)	m (g/l)	t (min)	K_F (mg/g)/(mg/l)$^{1/n}$	$1/n$	q_m (mg/g)	K_L (l/mg)	Reference
BFA	MG	7.0	30	5–250	1	240	25.149	0.423	170.33	0.148	[9]
ACC	MG	7.0	30	5–250	20	240	1.189	0.411	8.27	0.129	[9]
ACL	MG	7.0	30	5–250	4	240	5.629	0.449	42.18	0.117	[9]
BFA	CR	7.0	30	5–30	1	240	8.162	0.288	11.89	3.334	[10]
ACC	CR	7.0	30	5–30	20	240	0.402	0.234	0.635	1.867	[10]
ACL	CR	7.0	30	5–30	2	240	0.939	0.341	1.875	1.378	[10]
BFA	OG	4.0	30	5–30	2	240	3.084	0.544	18.77	0.177	[11]
BFA	MV	9.0	30	5–30	4	240	13.296	0.237	26.25	0.680	[11]
BFA	BG	3.0	15	50–300	3	300	14.832	0.616	133.33	0.095	[16]
BFA	BG	3.0	30	50–300	3	300	30.298	0.504	116.27	0.350	[16]
BFA	BG	3.0	45	50–300	3	300	36.503	0.479	114.76	0.529	[16]
CAC	MB	7.4	30	100–200	2	35	843.01	0.288	980.3	0.479	[17]
BDC	MB	7.4	30	100–200	10	35	1.992	0.514	143.2	0.120	[17]
CSC	MB	7.4	30	200–400	10	35	1.859	0.677	277.9	0.091	[17]
GSC	MB	7.4	30	200–300	10	35	2.010	0.524	164.9	0.128	[17]
RHC	MB	7.4	30	200–400	10	35	3.387	0.378	342.5	0.358	[17]
SC	MB	7.4	30	200–300	10	35	3.297	0.519	472.1	0.389	[17]
CAC	CR	7.4	30	200–400	4.6	35	2.450	0.493	493.8	0.023	[18]
BDC	CR	7.4	30	50–150	10	35	0.562	0.654	101.9	0.010	[18]
CSC	CR	7.4	30	75–175	10	35	0.879	0.585	188.4	0.014	[18]
GSC	CR	7.4	30	50–150	10	35	0.818	0.545	110.8	0.019	[18]
RHC	CR	7.4	30	75–175	10	35	0.633	0.578	237.8	0.012	[18]
SC	CR	7.4	30	75–175	10	35	0.853	0.771	403.7	0.0.10	[18]
CpAC	CR	2.0	35	0–20	10	40	2.530	0.295	6.72	0.18	[19]
PAC	RR 45	6.0	22	–	1.5	120	2.722	1.192	–	–	[26]
PAC	RG 8	6.0	22	–	1.5	120	2.005	0.795	–	–	[26]
PiAC	AB	5.4	30	0–400	1	4 days	–	–	589	–	[27]
PiAC	TB	6.5	30	0–400	1	5 days	–	–	983	–	[27]
PiAC	MB	6.6	30	0–400	1	5 days	–	–	484	–	[27]
AC	Safranin	–	32	–	0.2	2 days	165.5	0.240	576	0.065	[28]
AC	Safranin	–	40	–	0.2	2 days	106.3	0.312	564	0.039	[28]

Adsorbent—BFA: bagasse fly ash, ACC: commercial grade activated carbon, ACL: laboratory grade activated carbon, AC: activated carbon, PAC: powdered activated carbon, PiAC: pinewood activated carbon, CAC: commercial activated carbon, BDC: bamboo duct carbon, CSC: coconut shell carbon, GSC: groundnut shell carbon, RHC: rice husk carbon, SC: straw carbon, CpAC: coir-pith activated carbon. Adsorbate—BG: brilliant green, OG: orange-G, MV: methyl violet, CR: congo-red, MG: malachite green, RR 45: reactive red, and RG 8: reactive green, AB: astrazine blue, TB: telon blue, and MB: methylene blue.

3.6.2. Temkin isotherm

Temkin isotherm assumes that (i) the heat of adsorption of all the molecules in the layer decreases linearly with coverage due to adsorbate–adsorbate interactions and (ii) adsorption is characterized by a uniform distribution of binding energies, up to some maximum binding energy [8]. The Temkin isotherm is represented by following equation:

$$q_e = \frac{RT}{b}\ln(K_T C_e) \tag{14}$$

Eq. (14) can be expressed in its linear form as:

$$q_e = B_1 \ln K_T + B_1 \ln C_e \tag{15}$$

where

$$B_1 = \frac{RT}{b} \tag{16}$$

The adsorption data can be analyzed according to Eq. (15). A plot of q_e versus $\ln C_e$ enables the determination of the isotherm constants K_T and B_1. K_T is the equilibrium binding constant (l/mg) corresponding to the maximum binding energy and constant B_1 is related to the heat of adsorption.

3.6.3. Dubinin–Radushkevich isotherm

Another equation used in the analysis of isotherms was proposed by Dubinin and Radushkevich [11].

$$q_e = q_S \exp(-B\varepsilon^2) \tag{17}$$

where q_S is $D-R$ constant, and ε can be correlated:

$$\varepsilon = RT \ln\left(1 + \frac{1}{C_e}\right) \tag{18}$$

The constant B gives the mean free energy E of sorption per molecule of sorbate when it is transferred to the surface of the solid from infinity in the solution and can be computed using the following relationship:

$$E = \frac{1}{\sqrt{2B}} \tag{19}$$

Calculated $D-R$ isotherm constants as determined from the plot of $\ln q_e$ versus ε^2 (not shown here) for the adsorption of AO on BFA, ACC and ACL are shown in Table 3. From Table 3, it is clear that the sorption energy value is lowest for adsorption on ACL whereas it is highest for ACC adsorption. Also, q_S value is highest for BFA followed by ACL and ACC.

Since the calculated correlation coefficients (R^2) are also closer to unity for Langmuir model than that for any other isotherm model studied, therefore, the equilibrium adsorption data can be approximated more appropriately by the Langmuir isotherm model for the adsorption of AO by BFA, ACC and ACL. Fig. 9 depicts the comparison of experimental and predicted amount of AO adsorbed on BFA for all the isotherm models studied. Clearly, Langmuir isotherm best fits the experimental equilibrium data.

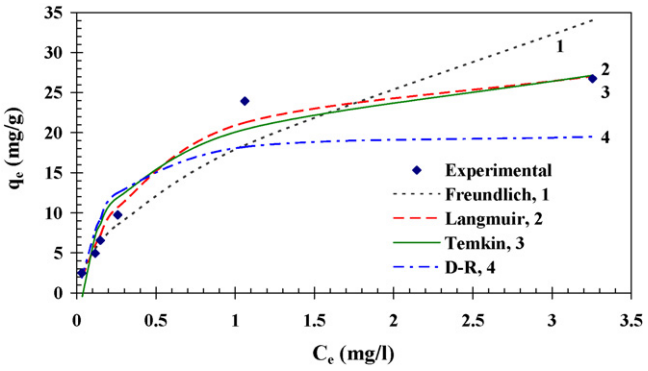

Fig. 9. Comparison of various isotherm equations for the adsorption of Auramine-O by BFA at 303 K.

3.7. Thermodynamic study

Thermodynamic data such as adsorption energy can be obtained from Langmuir and Temkin equation.

$$-\Delta G^0_{ads} = RT \ln(K) \tag{20}$$

where K is Langmuir or Temkin constant. For the Langmuir isotherm, the Gibbs free energy of adsorption for AO adsorption on BFA, ACC and ACL as calculated from Langmuir constant was found to be −33.56 kJ/mol, −37.15 kJ/mol and −33.35 kJ/mol, respectively. Thus adsorption on ACC (with a more negative value) is more favoured although other adsorbents have comparable values.

From constant K_T (Table 3), the Gibbs free energy of adsorption on BFA, ACC and ACL was found to be −34.81 kJ/mol, −35.85 kJ/mol and −35.29 kJ/mol, respectively. Interestingly, adsorption on ACC, again, has more negative values and thus, is more favoured. Also, ΔG values for both Tempkin and Langmuir isotherms are comparable.

4. Conclusion

The present study shows that the BFA is an effective adsorbent for the removal of (Auramine-O) AO from aqueous solution. Higher removal of AO by BFA, ACC and ACL was possible provided the initial adsorbate AO concentration was low in solution. The equilibrium between the bulk liquid phase AO concentration and the adsorbent surface concentration was practically achieved in 2 h. Adsorption kinetics followed second-order rate expression with initial sorption rate being highest for AO adsorption on BFA. The adsorption processes could well be described by two-stage diffusion. Langmuir isotherms showed favourable adsorptive removal of AO on all adsorbents studied. The cost and adsorption characteristics favour BFA to be used as an effective adsorbent for the removal of AO dye from aqueous solution.

Acknowledgement

Authors are thankful to the Ministry of Human Resource and Development, Government of India, for providing financial support to undertake the work.

References

[1] A. Martelli, G.B. Campart, R. Canonero, R. Carrozzino, F. Mattioli, L. Robbiano, M. Cavanna, Evaluation of auramine genotoxicity in primary rat and human hepatocytes and in the intact rat, Mutat. Res. 414 (1998) 37–47.

[2] IARC, Monographs on the Evaluation of Carcinogenic Risk to Humans, Supplement 7: Overall Evaluations of Carcinogenicity: an Updating of IARC Monographs, vols. 1–42, International Agency for Research on Cancer, Lyon, France, 1987, pp. 118–119.

[3] M.M. Nassar, Y.H. Magdy, Removal of different basic dyes from aqueous solutions by adsorption on palm-fruit bunch particles, Chem. Eng. J. 66 (1997) 223–226.

[4] G.M. Walker, L. Hansen, J.-A. Hanna, S.J. Allen, Kinetics of a reactive dye adsorption onto dolomitic sorbents, Water Res. 37 (2003) 2081–2089.

[5] G. McKay, Adsorption of dyestuffs from aqueous solutions with activated carbon. I. Equilibrium and batch contact-time studies, J. Chem. Technol. Biotechnol. 32 (1982) 759–772.

[6] S.J.T. Pollard, G.D. Fowler, C.J. Sollars, R. Perry, Low-cost adsorbents for waste and wastewater wastewater treatment: a review, Sci. Total Environ. 116 (1992) 31–32.

[7] I.D. Mall, S.N. Upadhaya, Y.C. Sharma, A review on economical treatment of wastewaters and effluents by adsorption, Intern. J. Environ. Studies 51 (1996) 77–124.

[8] V.C. Srivastava, M.M. Swamy, I.D. Mall, B. Prasad, I.M. Mishra, Adsorptive removal of phenol by bagasse fly ash and activated carbon: equilibrium, kinetics and thermodynamics, Colloid Surface A: Physicochem. Eng. Aspects 272 (2006) 89–104.

[9] I.D. Mall, V.C. Srivastava, N.K. Agarwal, I.M. Mishra, Adsorptive removal of malachite green dye from aqueous solution by bagasse fly ash and activated carbon- kinetic study and equilibrium isotherm analyses, Colloid Surface A: Physicochem. Eng. Aspects 264 (2005) 17–28.

[10] I.D. Mall, V.C. Srivastava, N.K. Agarwal, I.M. Mishra, Removal of congo red from aqueous solution by bagasse fly ash and activated carbon: kinetic study and equilibrium isotherm analyses, Chemosphere 61 (2005) 492–502.

[11] I.D. Mall, V.C. Srivastava, N.K. Agarwal, Removal of orange-G and methyl violet dyes by adsorption onto bagasse fly ash- kinetic study and equilibrium isotherm analyses, Dyes Pigments 69 (2006) 210–223.

[12] V.C. Srivastava, I.D. Mall, I.M. Mishra, Equilibrium modelling of single and binary adsorption of cadmium and nickel onto bagasse fly ash, Chem. Eng. J. 117 (2006) 79–91.

[13] L.S. Balistrieri, J.W. Murray, The surface chemistry of goethite (a-FeOOH) in major ion seawater, Am. J. Sci. 281 (6) (1981) 788–806.

[14] Y. Wong, J. Yu, Laccase catalysed decolorisation of synthetic dyes, Water Res. 33 (16) (1999) 3512–3520.

[15] Y.S. Ho, G. McKay, Pseudo-second order model for sorption processes, Process Biochem. 34 (1999) 451–465.

[16] V. Mane, I.D. Mall, V.C. Srivastava, Use of bagasse fly ash as an adsorbent for the removal of brilliant green dye from aqueous solution, Dyes Pigments, in press, doi:10.1016/j.jenvman.2006.06.024.

[17] K. Kannan, M.M. Sundaram, Kinetics and mechanism of removal of methylene blue by adsorption on various carbons—a comparative study, Dyes Pigments 51 (2001) 25–40.

[18] K. Kannan, M.M. Sundaram, Adsorption of congo red on various activated carbons, Water Air Soil Pollut. 138 (2002) 289–305.

[19] C. Namasivayam, D. Kavitha, Removal of congo red from water by adsorption onto activated carbon prepared from coir pith, an agricultural solid waste, Dyes Pigments 54 (2002) 47–58.

[20] W.J. Weber Jr., J.C. Morris, Kinetics of adsorption on carbon from solution, J. Sanitary Eng. Div. ASCE 89 (SA2) (1963) 31–59.

[21] J. Crank, The Mathematics of Diffusion, vol. 84, 1st ed., Oxford Clarendon Press, London, 1965.

[22] G. McKay, M.S. Otterburn, A.G. Sweeney, The removal of colour from effluent using various adsorbents. III. Silica: rate processes, Water Res. 14 (1980) 15–20.

[23] C. Aharoni, S. Sideman, E. Hoffer, Adsorption of phosphate ions by collod ion-coated alumina, J. Chem. Technol. Biotechnol. 29 (1979) 404–412.

[24] E. Tutem, R. Apak, C.F. Unal, Adsorptive removal of chlorophenols from water by bituminous shale, Water Res. 32 (1998) 2315–2324.

[25] S.D. Faust, O.M. Aly, Adsorption Processes for Water Treatment, Butterworths, 1987.

[26] S. Papic, N. Koprivanac, A.L. Bozic, A. Metes, Removal of some reactive dyes from synthetic wastewater by combined Al(III) coagulation/carbon adsorption process, Dyes Pigments 62 (2004) 293–300.

[27] R.L. Tseng, F.C. Wu, R.S. Juang, Liquid-phase adsorption of dyes and phenols using pinewood-based activated carbons, Carbon 41 (2003) 487–495.

[28] K.V. Kumar, S. Sivanesan, Comparison of linear and non-linear method in estimating the sorption isotherm parameters for safranin onto activated carbon, J. Hazard. Mater. B 123 (2005) 288–292.